

## CONCISE ARTICLE

View Article Online  
View Journal | View IssueCite this: *Med. Chem. Commun.*, 2014,  
5, 1533

## Identification and optimisation of 7-azaindole PAK1 inhibitors with improved potency and kinase selectivity†

William McCoull,<sup>a\*</sup> Edward J. Hennessy,<sup>\*b</sup> Kevin Blades,<sup>a</sup> Matthew R. Box,<sup>a</sup> Claudio Chuaqui,<sup>b</sup> James E. Dowling,<sup>b</sup> Christopher D. Davies,<sup>a</sup> Andrew D. Ferguson,<sup>b</sup> Frederick W. Goldberg,<sup>a</sup> Nicholas J. Howe,<sup>a</sup> Paul D. Kemmitt,<sup>a</sup> Gillian M. Lamont,<sup>a</sup> Katrina Madden,<sup>a</sup> Claire McWhirter,<sup>a</sup> Jeffrey G. Varnes,<sup>b</sup> Richard A. Ward,<sup>a</sup> Jason D. Williams<sup>a</sup> and Bin Yang<sup>b</sup>

A novel series of PAK1 inhibitors was discovered from a kinase directed screen. SAR exploration in the selectivity pocket and solvent tail regions was conducted to understand and optimise PAK1 potency and selectivity against targeted kinases. A liganded PAK1 crystal structure was utilised to guide compound design. Permeability and kinase selectivity impacted the translation of enzyme to cellular PAK1 potency. Compound **36** (AZ-PAK-36) demonstrated improved Gini coefficient, good PAK1 cellular potency and has utility as a tool compound for target validation studies.

Received 27th June 2014  
Accepted 7th August 2014

DOI: 10.1039/c4md00280f

www.rsc.org/medchemcomm

## Introduction

The p21-activated kinases (PAKs) are a family of six serine/threonine-specific intracellular protein kinases which are positioned at the intersection of several signaling pathways of importance in cancer progression.<sup>1,2</sup> The PAK family is divided into two subgroups based on sequence homology: group I (PAKs 1–3) and group II (PAKs 4–6). Group I PAKs have high sequence identity in the kinase domain and possess an auto-inhibitory domain which is relieved by binding of the GTP-binding proteins Rac or Cdc42, whilst group II PAKs have lower kinase domain homology and are not activated by Rho GTPases.<sup>3</sup> Group I PAKs are overexpressed in a wide variety of cancers and PAK1 is commonly overexpressed in breast tumours.<sup>4</sup> In tumours characterised by neurofibromatosis type 2 (NF2) inactivation, group I PAKs have been shown to be hyper-activated.<sup>5</sup> Consequently, small molecule inhibitors of group I PAKs may have therapeutic efficacy in tumours characterised by PAK activation.

There are relatively few published reports of PAK inhibitors, including the patent literature.<sup>6–10</sup> Potent PAK inhibition with high kinase selectivity has proven difficult to achieve due to the large and flexible nature of the catalytic pocket. The two most

widely used PAK1 inhibitors to date are PF-3758309 (ref. 11) and FRAX-597 (ref. 12) (Fig. 1), and they have both shown efficacy in a KRAS-driven tumour mouse model of skin cancer.<sup>13</sup> However both have sub-optimal kinase selectivity and indeed the former is an inhibitor of both group I and II PAKs. Thus, to understand the role of group I PAKs more fully in oncology, small molecules with improved potency and kinase selectivity are required. In this paper we report the discovery and optimisation of a novel 7-azaindole series of PAK1 inhibitors with improved selectivity.

## Results and discussion

A kinase focused subset screen (120 000 compounds) of the AstraZeneca compound collection was conducted, from which we identified 7-azaindole **1** as a modestly potent inhibitor of PAK1 with 14-fold selectivity over PAK4 (Table 1). This screening set consisted of compounds which had previously shown activity in at least one kinase assay and was filtered by lead-like properties followed by a diversity-based selection. We did not expect to obtain selectivity within each of the PAK families, and so PAK1 was utilised as our primary group I PAK target while

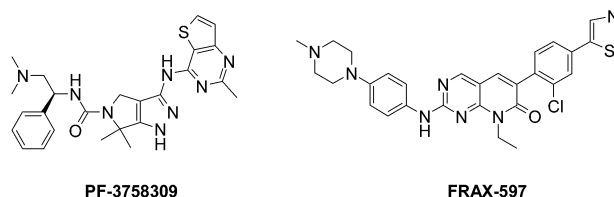
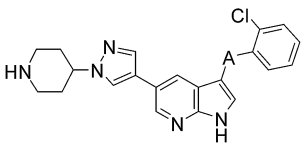


Fig. 1 Known PAK inhibitors.

<sup>a</sup>AstraZeneca, Alderley Park, Macclesfield, Cheshire, SK10 4TG, UK. E-mail: william.mccoull@astrazeneca.com; Tel: +44 (0)1625 519444<sup>b</sup>AstraZeneca, Gatehouse Park, Waltham, Massachusetts 02451, USA

† Electronic supplementary information (ESI) available: Synthetic details for the preparation of compounds, kinase selectivity data, and protein production/purification and X-ray crystallography conditions. See DOI: 10.1039/c4md00280f

Table 1 PAK1 and PAK4 potency for compounds 1–4

Cpd	A		
		PAK1 IC <sub>50</sub> <sup>a</sup> (μM)	PAK4 IC <sub>50</sub> <sup>a</sup> (μM)
1	CH <sub>2</sub>	0.083	1.2
2	C=O	0.018	0.55
3	—	0.46	0.17
4	SO <sub>2</sub>	6.3	>10

<sup>a</sup> Geometric mean of at least two experiments. IC<sub>50</sub> values were determined at ATP concentrations within 2-fold of the measured K<sub>M</sub> ATP for their respective kinases.

PAK4 was utilised as an anti-target to obtain selectivity against group II PAKs.<sup>14</sup> Gini coefficient<sup>15</sup> is commonly used to assess the kinase selectivity of a compound tested in a broad kinase panel, where a value between 0 and 1 is returned with more selective compounds having values closer to 1. An assessment of **1** revealed a low Gini coefficient of 0.29. 7-Azaindoles have previously been reported as kinase inhibitors, such as the marketed cancer drug vemurafenib which is an inhibitor of B-raf kinase (targeting V600E mutant).<sup>16</sup> In addition it has been reported that “selectively nonselective” 7-azaindoles were obtained for mixed lineage kinase 3,<sup>17</sup> indicating that kinase selectivity would be a key challenge for this chemotype. Consequently, potency and kinase selectivity became the main drivers for our lead optimisation efforts.

Initial chemistry explored the linker group between the 7-azaindole and aryl group (Table 1). The carbonyl linker in compound **2** afforded nearly 5-fold increase in PAK1 potency with an increase to 30-fold selectivity over PAK4. Removal of the linker altogether in **3** reduced potency 5-fold against PAK1 but increased PAK4 potency 7-fold. Sulfone linker **4** significantly reduced potency against both PAK1 and PAK4. The proposed conformation necessary for binding (based on later ligand-PAK1 crystal structure, Fig. 2) is an unfavourable conformation for the sulfone but favourable conformation for the other linkers. (see ESI†). Broader kinase screening of ketone **2** revealed a significantly improved kinase selectivity profile with Gini coefficient of 0.46, which encouraged us to maintain the carbonyl in all subsequent compounds.

The SAR of substitution around the phenyl ring was subsequently explored (Table 2). The chlorine of **2** was replaced with various *ortho* substituents in compounds **5–9** and all exhibited a decrease in PAK1 potency, with only methyl (**6**), fluoro (**7**) and the original chloro (**2**) compounds having greater potency than simple phenyl analogue **5**. As well as assessing PAK4 selectivity, we measured KDR and FGFR1 kinase inhibition.<sup>18</sup> Our lead compound **2** was not very selective against these additional kinases and neither is FRAX-597, thus we believed this data could be used to drive improvements in kinase selectivity. The chloro group was moved to the *meta* (**10**) and *para* (**11**)

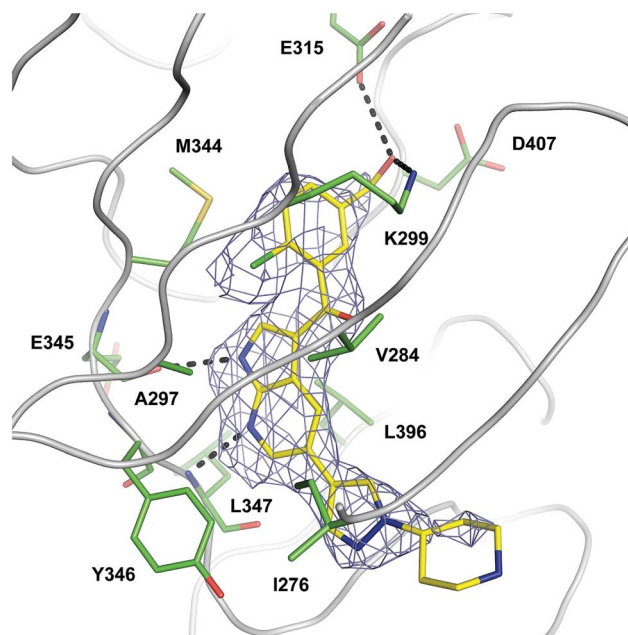
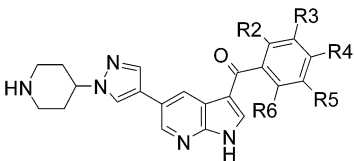


Fig. 2 Crystal structure of compound **15** in complex with the kinase domain of human PAK1 at 2.49 Å resolution. All residues located within 3.5 Å of the inhibitor are shown as green carbon sticks. Compound **15** is shown as yellow carbon sticks. The final 2Fo-Fc electron density map surrounding the inhibitor is shown as blue mesh (contoured at 1σ).

positions. The former led to 111-fold decrease in PAK1 potency while the latter was 14-fold less potent against PAK1. Selectivity against PAK4, KDR and FGFR1 decreased in both cases. Other groups at the *para* position were tolerated (**12**, **13**) and we decided to explore the combination of *ortho*-Cl with other substituents in compounds **14–24**. Di-*ortho* compound **14** maintained potency and selectivity but afforded no clear advantage over **2**. Di-substituted 2-chloro, 5-hydroxymethyl (**15**) was a successful attempt to introduce a substituent which would reduce lipophilicity, but isolipophilic 2-chloro, 5-cyano **16** was 10-fold less potent, suggesting the SAR is specific rather being driven by lipophilicity at this substituent. PAK1 potency could be increased by adding an appropriate substituent at the 5-position in combination with the 2-chloro group. Lipophilic groups such as halogen (**17** and **18**) maintained PAK1 potency and kinase selectivity as did the less lipophilic cyano analogue (**19**), which exhibited the best selectivity profile thus far. However, more polar groups (**20** and **21**) eroded PAK1 potency and alcohol **22** appeared to give the best potency/lipophilicity balance. Ethers (**23** and **24**) were tolerated and the larger phenyl ether **24** was not only more potent against PAK1 but also had significantly improved selectivity against PAK4. Compounds **22** and **24** were tested in a cellular PAK1 phosphorylation assay<sup>19</sup> and gave disappointing IC<sub>50</sub> values of 6.2 and 1.6 μM respectively. This larger than expected drop-off from enzyme to cell potency was attributed to low permeability as **22** and **24** had measured *P*<sub>app</sub> values of 0.14 and 0.11 × 10<sup>−6</sup> cm s<sup>−1</sup> respectively in a Caco-2 permeability assay.

We rationalised that the strongly basic piperidine, present in all compounds described so far, was contributing to low

Table 2 PAK1 potency and selectivity vs. PAK4, KDR and FGFR1 for compounds 2 and 5–24



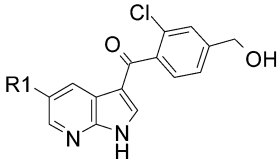
Cpd	R2	R3	R4	R5	R6	PAK1 IC <sub>50</sub> <sup>a</sup> (μM)	PAK4 selectivity <sup>a,b</sup>	KDR selectivity <sup>a,b</sup>	FGFR1 selectivity <sup>a,b</sup>	log D <sub>7.4</sub>
2	Cl	H	H	H	H	0.018	30	4.5	3	1.6
5	H	H	H	H	H	0.4	3.4	0.25	0.24	1.4
6	Me	H	H	H	H	0.063	—	2.7	0.56	1.8
7	F	H	H	H	H	0.12	6.7	0.68	0.57	1.5
8	CN	H	H	H	H	0.74	3.5	1.4	0.7	0.57
9	MeO	H	H	H	H	0.49	14	0.9	0.13	1.1
10	H	Cl	H	H	H	2	3	0.055	0.032	2.3
11	H	H	Cl	H	H	0.26	6.6 <sup>c</sup>	0.16	0.12	2.2
12	H	H	CH <sub>2</sub> OH	H	H	0.63	0.52	0.17	0.79	0.53
13	H	H	CH <sub>2</sub> OPh	H	H	0.084	90	0.42	1.9	3.2
14	Cl	H	H	H	Me	0.088	27	3.5	1.4	2.3
15	Cl	H	H	CH <sub>2</sub> OH	H	0.064	4.2	3.2	1.2	0.96
16	Cl	H	H	CN	H	0.65	8.3	1.5	0.49	1.1
17	Cl	H	F	H	H	0.013	50	9.8	4.2	2.1
18	Cl	H	Cl	H	H	0.0075	38	4.5	1.4	2.5
19	Cl	H	CN	H	H	0.023	36	11	7.4	1.2
20	Cl	H	CONH <sub>2</sub>	H	H	0.63	2.6	0.44	0.52	0.5
21	Cl	H	SO <sub>2</sub> Me	H	H	0.44	>23	1.5	3.2	0.63
22	Cl	H	CH <sub>2</sub> OH	H	H	0.0076	31	4.9	13	0.97
23	Cl	H	CH <sub>2</sub> OMe	H	H	0.021	56	2.0	2.5	1.7
24	Cl	H	CH <sub>2</sub> OPh	H	H	0.003	250	22	21	3.7

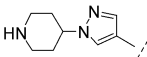
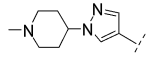
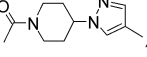
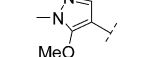
<sup>a</sup> Geometric mean of at least two experiments unless otherwise stated. IC<sub>50</sub> values were determined at ATP concentrations within 2-fold of the measured K<sub>M</sub> ATP for their respective kinases. <sup>b</sup> Selectivity calculated from ratio of IC<sub>50</sub> values. <sup>c</sup> *n* = 1.

permeability, thus we sought to modulate this part of the molecule (Table 3). Methylation of the piperidine (25) maintained potency and selectivity but did not improve permeability.

Acetylation of the piperidine (26) did reduce potency and selectivity somewhat but gave a 12-fold increase in permeability, confirming that variation of this substituent was important to

Table 3 PAK1 potency, selectivity vs. PAK4, KDR and FGFR1 and permeability for compounds 22 and 25–27



Cpd	R1	PAK1 IC <sub>50</sub> <sup>a</sup> (μM)	PAK4 selectivity <sup>a,b</sup>	KDR selectivity <sup>a,b</sup>	FGFR1 selectivity <sup>a,b</sup>	Permeability <i>P</i> <sub>app</sub> <sup>c</sup> (× 10 <sup>−6</sup> cm s <sup>−1</sup> )	log D <sub>7.4</sub>
22		0.0076	31	4.9	13	0.14	0.97
25		0.012	24	4.4	8.3	0.16	2.2
26		0.055	4	0.27	1.8	1.7	2.5
27		0.037	7.8	0.38	1.1	7.8	3.4

<sup>a</sup> Geometric mean of at least two experiments. IC<sub>50</sub> values were determined at ATP concentrations within 2-fold of the measured K<sub>M</sub> ATP for their respective kinases. <sup>b</sup> Selectivity calculated from ratio of IC<sub>50</sub> values. <sup>c</sup> Compounds were incubated at 10 μM in cultured human Caco-2 cells at pH 6.5.<sup>20</sup>

improving permeability. A further increase in permeability was obtained with truncated pyrazole analogue **27**, without any further erosion of potency and selectivity relative to **26**. This increased permeability correlates with increased lipophilicity and removal of the ionisable basic nitrogen.

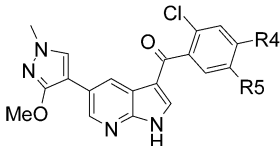
Next we combined the truncated methoxy-pyrazole with potent aryl substituents from our previous SAR exploration (Table 4). Extended ether **28** was not as potent as earlier analogue **24** but still exhibited high selectivity vs. PAK4. 2-Fluoro (**29**) and 2-aza (**30**) benzyl ethers gave similar encouraging PAK1 potency and PAK4 selectivity, but 3-aza analogue (**31**) was less potent and selective. Disappointingly, little selectivity was obtained for KDR or FGFR1 which correlated with poor overall kinase selectivity (Gini coefficient of 0.35 for **30**). Consequently we abandoned further work with these larger groups at the R4 position.

An earlier compound, **15**, was co-crystallised with the kinase domain of human PAK1. The resulting structure confirmed that the 7-azaindole formed a pair of hinge binding interactions with the back bone carbonyl of E345 and amide NH of L347, the pyrazole was positioned toward the solvent, and the chloro-aryl ring substituent was directed to the selectivity pocket and in front of the gatekeeper residue M344 (Fig. 2). On the opposing side of the aryl ring, the alcohol forms interactions with both residues K299 and E315. The length of these electrostatic interactions are not ideal given their bond distances of 3.3 Å to the side chain of residue K299 and 3.5 Å to the side chain of residue E315 (Fig. 2). We envisaged that reducing the distance between the alcohol and these catalytic residues would generate more favourable electrostatic interactions. Consequently, homologated alcohols **32** and **33** were prepared, and the latter demonstrated an 11-fold potency increase relative to **15**. Unfortunately, this potency increase was not sufficient to obtain selectivity against KDR and FGFR1. Thus, we decided to return to the *ortho*-Cl-phenyl selectivity pocket group and explore the solvent channel as an alternative path to improvements in potency and selectivity.

A diverse array of compounds with various groups intended to explore the solvent channel were prepared and bicycle **34** gave encouraging potency, including cellular potency, and selectivity similar to our original piperidine **2** (Table 5). Expansion to the 6,6-bicyclic systems improved potency in **35** and particularly in **36** which afforded the highest selectivity and cell potency of any compound from this series. The basic nitrogen appeared to be necessary since acetyl analogue **37** had significantly reduced potency. In **36**, we achieved improved selectivity against PAK4, KDR and FGFR1 compared to FRAX-597 (Table 5). In terms of broader kinase selectivity, **36** can be considered equally kinase selective with FRAX-597 given their Gini coefficients of 0.60 and 0.59 (ref. 13) respectively but with differing overall profile. Compound **36** exhibited >95% inhibition of 11/125 kinases tested at 0.1 μM: Abl1, Fyn, Lck, Lyn, PTK6, Ret, PAK1, Src and Yes1.

To understand the utility of **36** as an *in vitro* tool for target validation studies, appropriate cellular activity is important. The cell drop off due to increased ATP competition was calculated using the Cheng–Prusoff equation.<sup>21</sup> Based on the  $K_M$  of PAK1 for ATP (17 μM) and assuming that the compounds are fully competitive with ATP and a cellular ATP concentration of 2 mM, we anticipated a 75-fold drop-off from kinase potency to cell potency. In agreement with this, an excellent correlation ( $r^2 = 0.992$ ) was obtained for those compounds tested in both ATP concentration assays, which included 7-azaindoles and FRAX-597 (Fig. 3). In the absence of other factors, a similar correlation was expected between cell and enzyme potency. However, a larger spread of data was observed (Fig. 4). Compounds which exhibited higher drop-offs, such as **22** and **24** were characterised by low permeability, while compounds that exhibited lower drop-offs, such as **28–31** were characterized by poor kinase selectivity. Both compound **36** and FRAX-597 are close to the expected 75-fold drop-off between enzyme and cell potency. Compound **36** has a lower level of plasma protein binding (3.5% vs. 0.08% free) which is beneficial for use in cellular target validation experiments run in the presence of serum.

Table 4 PAK1 potency and selectivity vs. PAK4, KDR and FGFR1 for compounds 27–33



Cpd	R4	R5	PAK1 IC <sub>50</sub> <sup>a</sup> (μM)	PAK4 selectivity <sup>a,b</sup>	KDR selectivity <sup>a,b</sup>	FGFR1 selectivity <sup>a,b</sup>	log D <sub>7.4</sub>
27	CH <sub>2</sub> OH	H	0.037	7.8	0.38	1.1	3.4
28	CH <sub>2</sub> OPh	H	0.043	>240	2.1	3.9	>4.9
29	CH <sub>2</sub> O-2-F-Ph	H	0.048	>630	1.0	2.3	>4.1
30	CH <sub>2</sub> O-2-pyridyl	H	0.014	100	2.5	10	>4.3
31	CH <sub>2</sub> O-3-pyridyl	H	0.13	29	0.71	0.44	>4.3
32	CH <sub>2</sub> CH <sub>2</sub> OH	H	0.14	6.4	0.2	0.14	3.1
33	H	CH <sub>2</sub> CH <sub>2</sub> OH	0.0058	42	1.5	2.4	3.2

<sup>a</sup> Geometric mean of at least two experiments unless otherwise stated. IC<sub>50</sub> values were determined at ATP concentrations within 2-fold of the measured  $K_M$  ATP for their respective kinases. <sup>b</sup> selectivity calculated from ratio of IC<sub>50</sub> values.

Table 5 PAK1 potency and selectivity vs. PAK4, KDR and FGFR1 for compounds 2, 34–37 and FRAX-597

Cpd	R1	PAK1 IC <sub>50</sub> <sup>a</sup> (μM)	PAK4 selectivity <sup>a,b</sup>	KDR selectivity <sup>a,b</sup>	FGFR1 selectivity <sup>a,b</sup>	pPAK1 IC <sub>50</sub> <sup>a</sup> (μM)	log D <sub>7.4</sub>	h plasma protein binding (%free)
2		0.018	30	4.5	3	0.87	1.6	11
34		0.033	63	4.3	1.3	1.1	—	—
35		0.0045	180	18	4.3	0.65	4	3.4
36		0.0010	450	50	24	0.14	3.3	3.5
37		0.27	6.6	0.12	0.33	1.3	—	—
FRAX-597		0.0028	260	1.2	1.7	0.088	>4	0.08

<sup>a</sup> Geometric mean of at least two experiments unless otherwise stated. IC<sub>50</sub> values were determined at ATP concentrations within 2-fold of the measured K<sub>M</sub> ATP for their respective kinases. <sup>b</sup> selectivity calculated from ratio of IC<sub>50</sub> values.

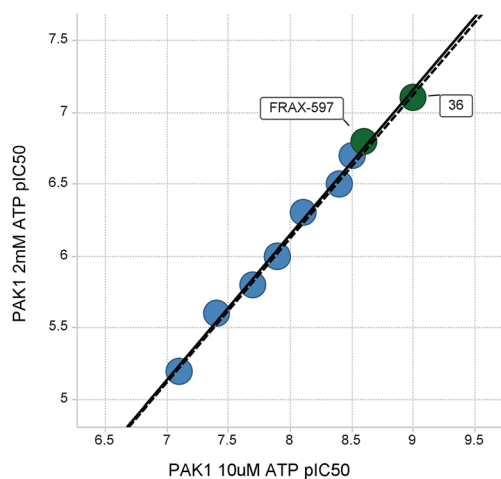


Fig. 3 PAK1 enzyme potency (2 mM ATP against 10 μM ATP) correlation with best fit (bold) and calculated IC<sub>50</sub> shift for ATP competitive compounds (dashed) lines shown.

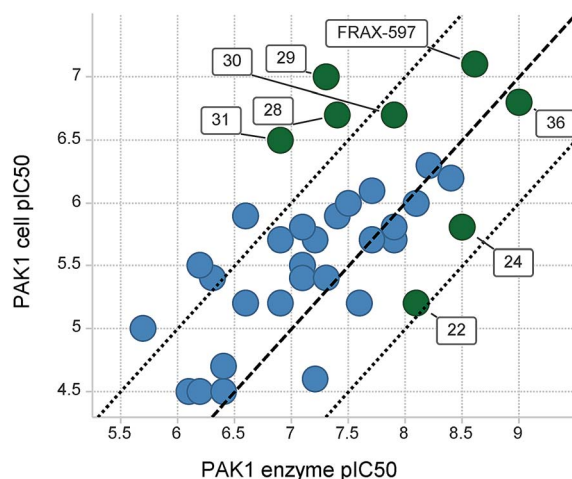


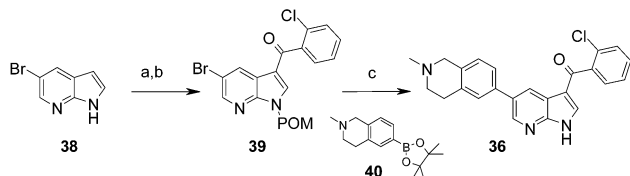
Fig. 4 PAK1 cell: enzyme correlation for 7-azaindoles and FRAX-597 with 1 : 10/100/1000 lines shown.

## Synthesis

A number of approaches were undertaken to synthesise the compounds studied, with routes to representative examples summarised in Schemes 1–3 (full details for all compounds are available in the ESI†). In the synthesis of compound 36, the aryl ketone was installed early by a Friedel–Crafts acylation between 5-bromo-7-azaindole 38 and 2-chlorobenzoyl chloride (Scheme 1). Subsequent deprotonation of the 7-azaindole with sodium

hydride and reaction with chloromethyl pivalate provided pivaloyloxymethyl (POM) protected 7-azaindole 39 in good yield. A Suzuki–Miyaura cross coupling with 40 followed by removal of the POM group with NaOH gave, after reverse phase purification, 36 in moderate yield. Intermediate 39 allowed facile exploration of the 5 position of the 7-azaindole. Variation of the boronate coupling partner in the Suzuki–Miyaura cross coupling reaction with 39 afforded the 7-azaindole compounds in Table 5.

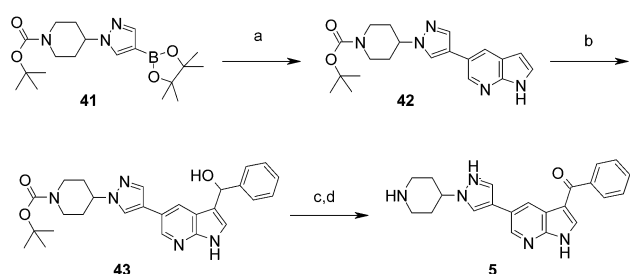




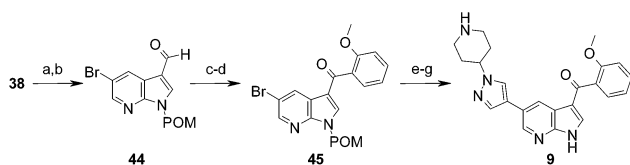
**Scheme 1** Reagents and conditions: (a)  $\text{AlCl}_3$ , 2-Cl-PhCOCl, DCM, 52%; (b) chloromethyl pivalate, NaH, DMF, 87%; (c) (i)  $\text{Pd}(\text{PPh}_3)_4$ ,  $\text{K}_2\text{CO}_3$ , 3 : 1 DME :  $\text{H}_2\text{O}$ , 75 °C, (ii) NaOH, MeOH, THF, 25% (2 steps).

Alternatively, the aryl ketone was installed late in the synthesis allowing variation of this group as in the synthesis of compound **5** (Scheme 2). The initial step was a Suzuki–Miyaura cross coupling between **38** and boronate **41** (ref. 22) which afforded **42** in excellent yield. Reaction of **42** with benzaldehyde and KOH in MeOH gave alcohol **43** in moderate yield. Subsequent oxidation to the ketone using  $\text{MnO}_2$  followed by treatment with acid to remove the butoxycarbonyl (Boc) group afforded **5**.

Further variations to the aryl ring were explored using a third route (Scheme 3). Key aldehyde intermediate **44** was synthesised in good yield from **38** in two steps. After protection with POM the aldehyde was installed under Vilsmeier–Haack conditions. It was possible to successfully react aldehyde **44** with various aryl lithium or Grignard reagents and ketone **45** was obtained in excellent yield from the latter after subsequent  $\text{MnO}_2$  oxidation. The pyrazole fragment was installed as previously in good yield. Compound **9** was then isolated after removal of POM and Boc protecting groups.



**Scheme 2** Reagents and conditions: (a) **38**,  $\text{Pd}(\text{dppf})\text{Cl}_2$ ,  $\text{K}_2\text{CO}_3$ , 10 : 1 DME :  $\text{H}_2\text{O}$ , 100 °C, 92%; (b) benzaldehyde, KOH, MeOH, 45%; (c)  $\text{MnO}_2$ , DCM 87%; (d) HCl, dioxane, 19%.



**Scheme 3** Reagents and conditions: (a) chloromethyl pivalate, NaH, DMF, 0 °C, 58%; (b)  $\text{POCl}_3$ , DMF, 0 to 50 °C, 70%; (c) 2-MeO-PhMgBr, THF, 97%; (d)  $\text{MnO}_2$ , DCM, 88%; (e) **41**,  $\text{Pd}(\text{dppf})\text{Cl}_2$ ,  $\text{K}_2\text{CO}_3$ , 10 : 1 DME :  $\text{H}_2\text{O}$ , 100 °C, 86%; (f) NaOH, MeOH, THF, 99%; (g) HCl, 1,4-dioxane, 35%.

## Conclusions

In summary, a novel 7-azaindole series of PAK1 inhibitors was identified. SAR exploitation enabled improvements in enzyme and cellular potency and kinase selectivity to afford **36** (AZ-PAK-36) as a useful tool compound for target validation experiments.

## Acknowledgements

Martina Fitzek, Renee Garcia-Arenas and Brenda McDermott are acknowledged for generating kinase inhibition data. Robert Godin, Mark Roth and Paul Clarkson are acknowledged for expert technical assistance in interpretation of biological data. Caroline Rivard and Christopher Jones are acknowledged for expert DMPK input.

## Notes and references

- 1 M. Radu, G. Semenova, R. Kosoff and J. Chernoff, *Nat. Rev. Cancer*, 2014, **14**, 13–25.
- 2 H. King, N. S. Nicholas and C. M. Wells, *Int. Rev. Cell Mol. Biol.*, 2014, **309**, 347–387.
- 3 R. Kumar, A. E. Gururaj and C. J. Barnes, *Nat. Rev. Cancer*, 2006, **6**, 459–471.
- 4 C. C. Ong, A. M. Jubbs, P. M. Haverty, W. Zhou, V. Tran, T. Truong, H. Turley, T. O'Brien, D. Vucic, A. L. Harris, M. Belvin, L. S. Friedman, E. M. Blackwood, H. Koeppen and K. P. Hoeflich, *Proc. Natl. Acad. Sci. U. S. A.*, 2011, **108**, 7177–7182.
- 5 C. W. Menges, E. Sementino, J. Talarchek, J. Xu, J. Chernoff, J. R. Peterson and J. R. Testa, *Mol. Cancer Res.*, 2012, **10**, 1178–1188.
- 6 C. Yi, J. Maksimoska, R. Marmorstein and J. L. Kissil, *Biochem. Pharmacol.*, 2010, **80**, 683–689.
- 7 J. J. Crawford, K. P. Hoeflich and J. Rudolph, *Expert Opin. Ther. Pat.*, 2012, **22**, 293–310.
- 8 Y. Xu, J. M. Foulks, A. Clifford, B. Brenning, S. Lai, B. Luo, K. M. Parnell, S. Merx, M. V. McCullar, S. B. Kanner and K. Ho, *Bioorg. Med. Chem. Lett.*, 2013, **23**, 4072–4075.
- 9 S. T. Staben, J. A. Feng, K. Lyle, M. Belvin, J. Boggs, J. D. Burch, C. Chua, H. Cui, A. G. DiPasquale, L. S. Friedman, C. Heise, H. Koeppen, A. Kotey, R. Mintzer, A. Oh, D. A. Roberts, L. Rouge, J. Rudolph, C. Tam, W. Wang, Y. Xiao, A. Young, Y. Zhang and K. P. Hoeflich, *J. Med. Chem.*, 2014, **57**, 1033–1045.
- 10 C. Guo, I. McAlpine, J. Zhang, D. D. Knighton, S. Kephart, M. C. Johnson, H. Li, D. Bouzida, A. Yang, L. Dong, J. Marakovits, J. Tikhe, P. Richardson, L. C. Guo, R. Kania, M. P. Edwards, E. Kraynov, J. Christensen, J. Piraino, J. Lee, E. Dagostino, C. Del-Carmen, Y. Deng, T. Smeal and B. W. Murray, *J. Med. Chem.*, 2012, **55**, 4728–4739.
- 11 B. W. Murray, C. Guo, J. Piraino, J. K. Westwick, C. Zhang, J. Lamerdin, E. Dagostino, D. Knighton, C. Loi, M. Zager, E. Kraynov, I. Popoff, J. G. Christensen, R. Martinez, S. E. Kephart, J. Marakovits, S. Karlicek, S. Bergqvist and T. Smeal, *Proc. Natl. Acad. Sci. U. S. A., Early Ed.*, 2010, 1–6.

- 12 S. Licciulli, J. Maksimoska, C. Zhou, S. Troutman, S. Kota, Q. Liu, S. Duron, D. Campbell, J. Chernoff, J. Field, R. Marmorstein and J. L. Kissil, *J. Biol. Chem.*, 2013, **288**, 29105–29114.
- 13 H. Y. Chow, A. M. Jubb, J. N. Koch, Z. M. Jaffer, D. Stepanova, D. A. Campbell, S. G. Duron, M. O'Farrell, K. Q. Cai, A. J. P. Klein-Szanto, J. S. Gutkind, K. P. Hoefflich and J. Chernoff, *Cancer Res.*, 2012, **72**, 5966–5975.
- 14 PAK1 and PAK4 kinase assays: the inhibitory activity of compound was determined by caliper off-chip incubation mobility shift assays, using a microfluidic chip to measure the conversion of fluorescent labeled peptide to a phosphorylated product. Fluorescently tagged peptide substrates were synthesized by Cambridge Research Biochemicals (Cleveland, U.K.). 12 point half-log compound concentration–response curves, with a top concentration of 100  $\mu\text{M}$  were generated from 10 mM stocks of compound solubilised in DMSO using an Echo 555 (Labcyte Inc., Sunnyvale, CA). All assays were preformed in white Greiner 384-well low volume plates (Greiner Bio-One, UK), in a total reaction volume of 12  $\mu\text{L}$  and 1% (v/v) final DMSO concentration. Enzymes and substrates were added separately to the compound plates and incubated at room temperature. The kinase reaction was then quenched by the addition of 10  $\mu\text{L}$  stop buffer (100 mM HEPES pH 7.5, 5% v/v DMSO, 44 mM EDTA, 0.22% v/v CR-3 0.033% Brij35). Stopped assay plates were read using a Caliper LabChip EZ reader (PerkinElmer Waltham, MA).  $\text{IC}_{50}$  values were calculated using Genedata Screener (Genedata AG, Basel, Switzerland). PAK1 kinase domain was purchased from Abcam (Cambridge, U.K.). The kinase reaction (10  $\mu\text{M}$ /2 mM ATP, 25 pM PAK1, 1  $\mu\text{M}$  peptide substrate 5-FAM-KPDRKKRYTVVGNPY-amide) in phosphorylation buffer (50 mM HEPES pH 7.3, 10 mM  $\text{MgCl}_2$ , 1 mM DTT 0.01% Tween20, 0.05  $\text{mg mL}^{-1}$  BSA) was quenched after a 120 min incubation. PAK4 kinase domain was purchased from Life Technologies (Thermo Fisher Scientific, Waltham, MA). The kinase reaction (1.5  $\mu\text{M}$  ATP, 2 nM PAK4, 1  $\mu\text{M}$  peptide substrate 5-FAM-Ahx-KKRNRRRLSVA-amide) in phosphorylation buffer (50 mM HEPES pH 7.3, 10 mM  $\text{MgCl}_2$ , 1 mM DTT 0.01% Tween20, 0.05  $\text{mg mL}^{-1}$  BSA) was quenched after a 90 min incubation.
- 15 P. P. Graczyk, *J. Med. Chem.*, 2007, **50**, 5773–5779.
- 16 G. Bollag, J. Tsai, J. Zhang, C. Zhang, P. Ibrahim, K. Nolop and P. Hirth, *Nat. Rev. Drug Discovery*, 2012, **11**, 873–886.
- 17 V. S. Goodfellow, C. J. Loweth, S. B. Ravula, T. Wiemann, T. Nguyen, Y. Xu, D. E. Todd, D. Sheppard, S. Pollack, O. Polesskaya, D. F. Marker, S. Dewhurst and H. A. Gelbard, *J. Med. Chem.*, 2013, **56**, 8032–8048.
- 18 R. A. Norman, A. Schott, D. M. Andrews, J. Breed, K. M. Foote, A. P. Garner, D. Ogg, J. P. Orme, J. H. Pink, K. Roberts, D. A. Rudge, A. P. Thomas and A. G. Leach, *J. Med. Chem.*, 2012, **55**, 5003–5012.
- 19 PAK1 phosphorylation cellular assay: cryopreserved MCF10A cells which have been transfected with PAK1 under control of a doxocycline inducible promoter were used. PAK expression was induced prior to cryopreservation. Revived cells were seeded with 3000 cells per well of a black 384 well plate and treated with compound for 2 h at 37  $^{\circ}\text{C}$ , 5%  $\text{CO}_2$ . After fixing with 4% paraformaldehyde and blocking of non-specific binding with a solution (1% BSA + 5% goat serum + 0.3% TritonX100 in PBS) the plates were treated with a phosphoPAK (Ser144) specific antibody and a secondary antibody labelled with Alexa Fluor-488 and Hoechst 33342. Between all reagent steps, the cells were washed with PBS. The stained cells were imaged on a Cellomix ArrayScan VTI using Mean Ring spot Average Intensity analysis method.
- 20 B. Over, P. McCarren, P. Artursson, M. Foley, F. Giordanetto, G. Groenberg, C. Hilgendorf, M. D. Lee, P. Matsson, G. Muncipinto, M. Pellisson, M. W. D. Perry, R. Svensson, J. R. Duvall and J. Kihlberg, *J. Med. Chem.*, 2014, **57**, 2746–2754.
- 21 A. C. Cheng, J. Eksterowicz, S. Geuns-Meyer and Y. Sun, *J. Med. Chem.*, 2010, **53**, 4502–4510.
- 22 A. B. Northrup, M. H. Katcher, M. D. Altman, M. Chenard, M. H. Daniels, S. V. Deshmukh, D. Falcone, D. J. Guerin, H. Hatch, C. Li, W. Lu, B. Lutterbach, T. J. Allison, S. B. Patel, J. F. Reilly, M. Reutershan, K. W. Rickert, C. Rosenstein, S. M. Soisson, A. A. Szewczak, D. Walker, K. Wilson, J. R. Young, B. Pan and C. J. Dinsmore, *J. Med. Chem.*, 2013, **56**, 2294–2310.